# Calibration of the isomer shift of 57Fe

Helvetica Physica Acta
Vol. 46, 1973.

Birkhäuser Verlag Basel

# Calibration of the Isomer Shift of $^{57}$Fe

by **P. Rüegsegger** and **W. Kündig**
Physik-Institut der Universität Zürich, Switzerland

(27. X. 72)

*Abstract.* The influence of the chemical environment on the lifetime of the 14.4 keV state in $^{57}$Fe was measured. The result, together with Mössbauer measurements, determined the change in the charge radius between the excited and the ground state as $\Delta R/R = -(3.1 \pm 0.5) \times 10^{-4}$.

## 1. Introduction

The hyperfine interaction measures the deviation from the Coulomb law for interactions between a nucleus and its surrounding electrons. Since a point charge characterizes the Coulomb force field, the hyperfine interaction is due to the deviation of the nucleus from a point charge. The field and the charge-current distribution are conventionally expanded in multipoles. The multipoles to be considered are the electric monopole, the magnetic dipole, the electric quadrupole, etc. The monopole interaction to be investigated in this article is proportional to the product of the electron density at the nucleus $|\psi(0)|^2$ and the mean square charge radius of the nucleus $\langle r_N^2 \rangle$. A manifestation of this interaction is the isomer shift (IS) as measured, e.g., in Mössbauer spectroscopy. The IS is due to differences in the chemical surroundings of the emitting and absorbing nuclei and due to the change in nuclear charge radius during the $\gamma$-transition

$$\mathrm{IS} \propto \Delta\langle r_N^2 \rangle \cdot \Delta|\psi(0)|^2. \tag{1}$$

Both $\Delta\langle r_N^2 \rangle$ and $\Delta|\psi(0)|^2$ are of considerable interest for nuclear and solid state physics. While the measurement of the IS is straightforward, the interpretation of the result is, except for qualitative arguments, almost impossible, although many investigators have tried to calculate under various assumptions the corresponding electron density differences.

The present paper describes the first experimental determination of $\Delta\langle r_N^2 \rangle$ for the most widely used 'Mössbauer nucleus' $^{57}$Fe. The experiment uses the fact that the coefficient for internal conversion of the M1 transition in $^{57}$Fe is proportional to the electron density $|\psi(0)|^2$. By measuring the influence of the chemical environment on the radioactive transition probability it is possible to determine via the conversion coefficient $\Delta|\psi(0)|^2$ and thus together with an IS measurement $\Delta\langle r_N^2 \rangle$. This experimentally

determined value of $\Delta\langle r_N^2\rangle$ may be used as a calibration constant to evaluate the great number of $^{57}$Fe IS measurements.

In the first part a survey is given on the present status of the $^{57}$Fe IS calibration. Then the relevant theories for the IS and the internal conversion are sketched. In the experimental part a coincidence technique to determine the changes of the radioactive half-life caused by the chemical environment is described.

## 2. Status of the Isomer Shift Calibration of $^{57}$Fe

Since the discovery of the IS by Kistner and Sunyar [1] in 1960 many investigators have tried to separate the nuclear and electronic factor in the expression for the IS. Most of these calibrations were done by calculating the electron density at the nucleus using Watson's Hartree–Fock calculations for the free ion wave functions [2], but differing in the assumptions made concerning the electron configuration in selected reference compounds. In a paper by Walker, Wertheim and Jaccarino [3] it was assumed that for ionic ferrous and ferric compounds the configurations $3d^6 4s^0$ and $3d^5 4s^0$ may be used. On this basis the authors obtained for the change in nuclear charge radius for the Mössbauer transition in $^{57}$Fe $\Delta R/R = -1.8 \cdot 10^{-3}$ (see definition of $\Delta R/R$, equation (3)). If the non-relativistic electron densities are corrected to the relativistic charge densities this value becomes $-1.2 \cdot 10^{-3}$ [4, 5]. The contribution of $4s$ electrons was estimated by Gol'danskii. The configuration used was $3d^{8-\eta-x}4s^x$, where $\eta$ is the effective charge on the individual atom taken from X-ray data. The value obtained was $\Delta R/R = -5 \cdot 10^{-4}$ [6]. These data were refined by Danon [7] by taking $s,s$ shielding into account. The value obtained was $-1.1 \cdot 10^{-3}$. This result was further refined by the introduction of a hybridization of the bonding orbitals for octahedral iron complexes and the shielding of the $4s$ electrons not only by the $3d$, but also by the $4p$ electrons. The value calculated was $\Delta R/R = -9.10^{-4}$. A different approach was taken by Šimánek et al. [8, 9]. The authors calculated $s$ electron densities in oxides and fluorides, taking into account the overlap of the iron $s$ electrons with the oxygen and fluorine $p$ electrons. By evaluating high pressure Mössbauer measurements by Drickamer et al. [10–12] the authors calculated $\Delta R/R = -4.0 \cdot 10^{-4}$ and $-5.2 \cdot 10^{-4}$ respectively. All the described theoretical approaches to the calibration have had the drawback that free ion wave functions had to be used in solids and many assumptions had to be made about the electronics tate. Partially these difficulties were overcome by McNab et al. [13]. By evaporating Fe simultaneously with noble gases, Mössbauer absorbers could be produced in which the Fe was assumed to be in the atomic state $3d^6 4s^2$. By measuring the 'free' atoms relative to $FeF_2$, which is 'known' to be in the state $3d^6 4s^0$ a value of $\Delta R/R = -9.1 \cdot 10^{-4}$ was obtained. This method was further refined by assuming that $^{57}$Co decays in solid xenon into Fe ($3d^6 4s^2$) and $Fe^+$ ($3d^7$). From the measured shift between the Fe and $Fe^+$ absorption peaks a value of $\Delta R/R = -8.7 \cdot 10^{-4}$ was calculated [14]. An interesting approach was used by Pleiter and Kolk [15] and Fujioka and Hisatake [16]. By measuring the ratio of the conversion coefficients $\alpha_{N_1}/\alpha_{M_1}$ for different chemical compounds and assuming that the difference of the electron densities of the nucleus in the compounds investigated is only due to the $4s$ shell, the authors calculated $\Delta R/R = -4.5 \cdot 10^{-4}$ and $-6 \cdot 10^{-4}$ respectively. From these examples of the wide range of calculated $\Delta R/R$ values and the many arguments which have to be used to justify the individual results it has to be concluded that the problem of IS calibration in $^{57}$Fe is still open.

## 3. Theory

*A. Isomer shift*

The electrostatic interaction between the nucleus and the electrons may be written as

$$W = \int \rho_N V \, d\tau, \tag{2}$$

where $\rho_N$ is the nuclear charge density and $V$ the potential of the electrons. $V$ may be expanded in a Taylor series about the origin

$$V = V_0 + V_x \cdot x + V_y \cdot y + V_z \cdot z + \tfrac{1}{2}(V_{xx} \cdot x^2 + V_{yy} \cdot y^2 + V_{zz} \cdot z^2) + V_{xy} \cdot xy + V_{yz} \cdot yz + V_{zx} \cdot zx + \ldots.$$

For a pure monopole form of $\rho_N$ one gets

$$W = V_0 \int \rho_N \, d\tau + \tfrac{1}{6}(V_{xx} + V_{yy} + V_{zz}) \int \rho_N r_N^2 \, d\tau$$

$$= V_0 \, Ze + \frac{2\pi}{3} Ze^2 |\psi(0)|^2 \langle r_N^2 \rangle,$$

where the Laplace equation $\Delta V = V_{xx} + V_{yy} + V_{zz} = 4\pi e |\psi(0)|^2$ was used. $Ze$ is the nuclear charge. The first term corresponds to the Coulomb energy of a point nucleus. The second term is the monopole interaction to be considered here. If one assumes a constant charge density inside a sphere of radius $R$ and zero outside ($\langle r_N^2 \rangle = \frac{3}{5} R^2$) the monopole interaction may be written as

$$W_1 = \frac{2\pi}{5} Ze^2 R^2 |\psi(0)|^2. \tag{3}$$

In Mössbauer spectroscopy the transition energies of an isotope in two chemically different environments are compared. The observed shift of the resonance line is

$$\mathrm{IS} = \frac{2\pi}{5} Ze^2 [R_{\mathrm{ex}}^2 - R_{\mathrm{gd}}^2][|\psi_a(0)|^2 - |\psi_s(0)|^2] \tag{4}$$

$R_{\mathrm{ex}}$ and $R_{\mathrm{gd}}$ are the nuclear radii in the excited and ground state, $|\psi_a(0)|^2$ and $|\psi_s(0)|^2$ are the electron densities at the nucleus for absorber and source. To a good approximation one may write

$$\mathrm{IS} = \frac{4\pi}{5} Ze^2 R^2 \frac{\Delta R}{R} \Delta |\psi(0)|^2, \tag{5}$$

where

$$\Delta R = R_{\mathrm{ex}} - R_{\mathrm{gd}} \quad \text{and} \quad R \approx R_{\mathrm{ex}} \approx R_{\mathrm{gd}}.$$

In this classical derivation the assumptions used are a) the electron density $|\psi(0)|^2$ is a constant over the nuclear volume, b) the change in electron density has no influence on the nuclear charge distribution and vice versa.

The electron charge density near the origin may be expanded in a power series

$$|\psi(r)|^2 = |\psi(0)|^2 (1 - b_1 r^2 + b_2 r^4 + \ldots). \tag{6}$$

The presence of the additional terms leads to the expression

$$\mathrm{IS} = \frac{2\pi}{3} Ze^2 \Delta |\psi(0)|^2 (\Delta\langle r_N^2\rangle - B_4 \Delta\langle r_N^4\rangle + B_6 \Delta\langle r_N^6\rangle + \ldots). \tag{7}$$

The error due to the non-uniformity of the electron density over the nuclear volume was calculated by Fricke and Waber to be 1% for $_{26}$Fe and 11% for $_{93}$Np [17]. Due to the smallness of the correction, higher order moments are usually not taken into account in evaluating Mössbauer IS measurements. However, the higher moments become very pronounced in muonic atoms. A comparison of IS measurements by muons with Mössbauer measurements is still ambiguous.

The second assumption is that the electron density has no influence on the nuclear charge distribution and vice versa. The influence of the electrons on the nuclear charge is called the polarization effect. From simple arguments one expects that the electrons reduce the repulsive force between the protons by screening and thus increase the binding energy of the protons. Mang et al. [18] showed for pure rotational transitions that the IS is identical to the polarization effect. For other transitions the polarization effect is believed to be negligible although the justifications for this are rather vague [19]. The additional question concerning the influence of the different nuclear charge distributions on the electron density was discussed by Fricke and Waber [17] and found to be negligible.

### *B. Internal conversion*

The conversion coefficient $\alpha = N_e/N_\gamma$ is the ratio between the number of electrons and the number of $\gamma$-quanta emitted in a nuclear decay. According to the shell from which the electron is taken, one introduces the partial conversion coefficients: $\alpha = \alpha_K + \alpha_{L_I} + \alpha_{L_{II}} + \alpha_{L_{III}} + \alpha_{N_I} + \ldots$. The possibility of decay of an excited state by internal conversion adds to the decay constant, thus the total decay constant $\lambda$ is equal to the sum of the partial decay constants $\lambda_\gamma$ and $\lambda_e$ for $\gamma$-emission and conversion electron emission.

$$\lambda = \lambda_\gamma + \lambda_e = \lambda_\gamma(1 + \alpha). \tag{8}$$

The internal conversion coefficient $\alpha$ for M1 transitions is for all shells within 1% proportional to the corresponding electron densities at the nucleus [20]. Detailed relativistic Hartree–Fock–Slater calculations by Raff, Alder and Bauer [21] are summarized in Table I. An indication of the reliability of these calculations is the good agreement found between the calculated and measured conversion coefficient.

$$\alpha_{\mathrm{theor.}} = 8.57$$

$$\alpha_{\mathrm{exp}} = 8.26 \pm 0.19 \quad [22]$$

$$\alpha_{\mathrm{exp}} = 8.19 \pm 0.18 \quad [23]$$

The last column of Table I shows that $\alpha_{i_S}$ is within 1% proportional to $|\psi_{i_S}(0)|^2$. If the small contributions of $p$ and $d$ electrons to the conversion coefficient are not taken into account, one may write

$$\alpha \propto |\psi(0)|^2$$

Table I

Internal conversion coefficients for the 14.4 keV transition in $^{57}$Fe: The calculated conversion coefficients $\alpha_i$ are collected for the different shells for the 14.4 keV transition in $^{57}$Fe. Column 3 gives the electron densities at the nucleus in atomic units (1 a.u. = $6.75 \cdot 10^{24}$ cm$^{-3}$). In the last column $\alpha_i/|\psi_i(0)|^2$ is given for $s$ shells.

| Shell | $\alpha_i$ | $\lvert\psi_i(0)\rvert^2$ (a.u.) | $\frac{\alpha_i}{\lvert\psi_i(0)\rvert^2}$ |
|---|---|---|---|
| $K_I$ | 7.675(0) | 1.335(+4) | 5.751(−4) |
| $L_I$ | 7.223(−1) | 1.258(+3) | 5.740(−4) |
| $L_{II}$ | 4.380(−2) | 6.800(0) | — |
| $L_{III}$ | 1.774(−2) | 6.196(−4) | — |
| $M_I$ | 1.064(−1) | 1.846(+2) | 5.765(−4) |
| $M_{II}$ | 6.107(−3) | 8.774(−1) | — |
| $M_{III}$ | 2.447(−3) | 8.004(−5) | — |
| $M_{IV}$ | — | 1.631(−8) | — |
| $M_V$ | — | 1.470(−13) | — |
| $N_I$ | 4.900(−3) | 8.642(0) | 5.670(−4) |

and

$$\frac{\Delta\lambda}{\lambda} = \frac{\Delta|\psi(0)|^2}{|\psi(0)|^2} \cdot \frac{\alpha}{\alpha+1} \cdot \tag{9}$$

*C. The calibration constant*

Both, the IS and the relative change of the decay constant $\Delta\lambda/\lambda$ are proportional to $\Delta|\psi(0)|^2$. By measuring the IS and $\Delta\lambda/\lambda$ on two chemically different samples it is possible to eliminate $\Delta|\psi(0)|^2$ and to get the calibration constant

$$\frac{\Delta R}{R} = \frac{5}{4\pi} \cdot \frac{\alpha}{\alpha+1} \cdot \frac{1}{Ze^2 R^2 |\psi(0)|^2} \cdot \frac{\mathrm{IS}}{\Delta\lambda/\lambda} \cdot \tag{10}$$

For the nuclear radius elastic electron scattering results on $^{56}$Fe were used [22]. The relation $R \propto A^{1/3}$ was used to correct the $^{56}$Fe value for $^{57}$Fe to obtain $R = (4.87 \pm 0.09)$ fm. The conversion coefficient used is $\alpha = 8.3 \pm 0.2$. The total electron density as calculated with a relativistic Hartree–Fock–Slater program is $|\psi(0)|^2 = 14{,}800$ a.u. (1 atomic unit is equal to the inverse cube of the Bohr radius, 1 a.u. = $6.75 \cdot 10^{24}$ cm$^{-3}$). According to Raff et al. the maximum uncertainty in the value of $|\psi(0)|^2$ is 5%.

## 4. Measurements

In order to determine the calibration constant $\Delta R/R$ for $^{57}$Fe one has to measure for two chemically different prepared sources the relative IS and the change in the decay constant $\Delta\lambda/\lambda$. Since the expected changes in the decay constants are rather small ($\Delta\lambda/\lambda \approx 10^{-4}$) and susceptible to systematic errors, all together four samples were used. The resulting six differences $\Delta\lambda/\lambda$ should be proportional to the respective IS. First, the choice of the matrix materials for the sources will be discussed, then the time measurements and the IS determination with their appropriate corrections are described.

*A. The four sources*

The decay scheme of $^{57}$Fe is shown in Figure 1. The 14.4 keV Mössbauer level to be investigated decays with a half-life of $T_{1/2} = 98.5 \pm 0.5$ ns [25, 26].

The choice of the matrices for $^{57}$Co has to meet several requirements. First, the IS between the sources should be as large as possible so that the small life-time differences become measurable. Second, the matrices are not allowed to contain $^{57}$Fe, so that self-absorption effects become negligible. Third, the ratio of the 14.4 keV $\gamma$-ray intensity to the 122 keV $\gamma$-ray intensity in the different sources should be approximately the same. The total absorption should therefore be negligibly small.

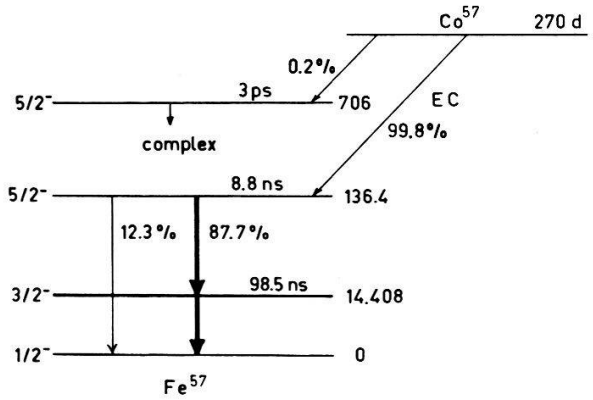


Figure 1
Decay scheme of $^{57}$Co.

The most serious restrictions are self-absorption effects. This may be understood from a classical treatment of emission and dispersion. The electric field of the $\gamma$ radiation is

$$E = E_0 \exp(-i(kx - \omega_0 t)) \exp(-\lambda t/2)$$

$$= E_0 \exp(-ikx) \frac{1}{2\pi i} \int_{-\infty}^{+\infty} \exp(i\omega t)\, d\omega/(\omega - \omega_0 - \tfrac{1}{2}i\lambda) \tag{11}$$

$$= E_0 \exp(-ikx) \int_{-\infty}^{+\infty} a(\omega) \exp(i\omega t)\, d\omega. \tag{12}$$

If the radiation passes through an $^{57}$Fe absorber with the resonance frequency $\omega_0$, each monochromatic component $a(\omega)$ excites forced oscillations of the resonators in the medium. These forced oscillations cause a polarization of the medium which is conveniently described by a complex refractive index

$$n = \frac{ck}{\omega} = (1 + r/(\omega_0^2 - \omega^2 + i\omega\lambda))^{1/2}. \tag{13}$$

The effect of passage through the absorber is to change $a(\omega)$ to $a'(\omega)$

$$a'(\omega) = a(\omega) \exp(-2ib\omega/(\omega_0^2 - \omega^2 + i\omega\lambda)). \tag{14}$$

The constant $b$ may be determined by the observed transmission at the center of the line

$$a'(\omega_0) = a(\omega_0) \exp(-2b/\lambda). \tag{15}$$

By combining equations (12) and (14) the time dependence of the transmitted amplitude is found to be

$$E' = E_0 \exp(-ikx) \frac{1}{2\pi i} \int_{-\infty}^{+\infty} \exp(i\omega t) \cdot \exp(2ib\omega/(\omega^2 - \omega_0^2 - i\omega\lambda))\, d\omega/(\omega - \omega_0 - \tfrac{1}{2}i\lambda). \tag{16}$$

The solution of this integral gives for the time dependence of the intensity [27]

$$I = I_0 \exp(-\lambda t)[J_0((\beta\lambda t)^{1/2})]^2, \tag{17}$$

where $J_0$ is the zero-order Bessel function.

The factor $\beta$ is given by

$$\beta = N\sigma_0 f, \tag{18}$$

where $N$ is the number of $^{57}$Fe atoms per cm$^2$, $\sigma_0 = \lambda^2/(\pi(1+\alpha))$ is the $^{57}$Fe cross-section for absorption ($\sigma_0 = (2.56 \pm 0.05)\ 10^{-18}$ cm$^2$) [28] and $f$ the recoil-free factor. The

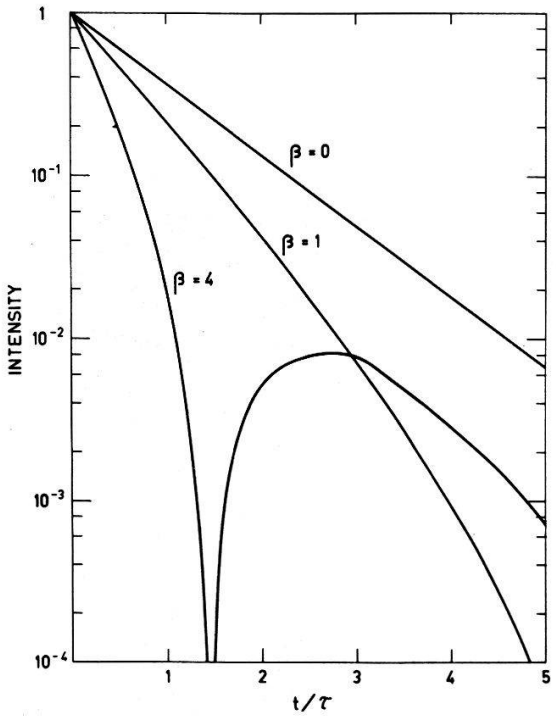


Figure 2
Time dependence of radiation after transmission through a resonance filter. The parameter $\beta$ corresponds to the resonance absorption at the centre of the line ($I = I_0 \exp(-\beta)$). The recoil-free factor is assumed to be one.

time dependence of the transmitted intensity for $f = 1$ and $\beta = 0, 1, 4$ is shown in Figure 2. It is evident that self-absorption may alter the result significantly. To determine an upper limit for the $^{57}$Fe impurity in the matrices one expands equation (17)

$$I = I_0 \exp(-\lambda t)(1 - \beta\lambda t/4 + \ldots). \tag{19}$$

In order to determine $\Delta\lambda/\lambda$ with an accuracy of $10^{-5}$ one requires $\beta < 4.10^{-5}$ or, according to (**18**), $N < 2.10^{13}$ $^{57}$Fe atoms/cm$^2$. The tolerable natural Fe impurity in a 1 mg/cm$^2$ matrix is $\approx 10^{-4}$. From these considerations it is evident that sources using Fe compounds are not feasible, even though they would be preferable from the point of view of large IS and ease in preparation. The $^{57}$Fe concentration in the sources due to the decaying $^{57}$Co is negligible (a 10 $\mu$C/cm$^2$ source produces per month $10^{11}$ $^{57}$Fe atoms/cm$^2$).

Chosen as matrices were: Co, Cu, Au and CoO. A 1 mg/cm$^2$ Cu foil was electroplated from a bath of 1.85 g $CuSO_4$ in 10 ml $H_2O$ and 0.83 ml $H_2SO_4$ (conc.) with a Pt anode. Similarly, the Co foil was plated from a bath of 0.75 g $CoCl_2 \cdot 6H_2O$, 0.9 g $CaCl_2$ and 5 ml $H_2O$ [29]. As cathodes, Fe foils etched with chromic acid were used. Under water the plated foils could be removed from the backing with a razor blade. The Au foil (0.1 mg/cm$^2$) was prepared by evaporating Au on a glass plate treated with a detergent (TEEPOL). It could be separated from the support similarly to the other foils. The unsupported foils were treated with insulin on an area of 0.1 cm$^2$, then approximately 20 $\mu$C $^{57}$Co in $H_2O$ was added. Insulin helps to avoid the formation of large crystals in drying. The $^{57}$Co was diffused into the foils in flowing $H_2$ at temperatures of $\approx$100 C below the melting point. The foils which were cleaned from undiffused $^{57}$Co were glued between a mylar and an Al foil. The cobaltous oxide exists in two forms CoO I and CoO II [30]. The form CoO I shows a narrow $Fe^{2+}$ line in the Mössbauer spectrum, contrary to CoO II in which $^{57}$Co decays into $Fe^{3+}$. The radioactive CoO I was prepared by New England Nuclear in Boston. The powder was put through a 5 $\mu$m mesh sieve on a layer of glue and then mounted between Al and mylar foils.

### *B. Lifetime measurements*

The lifetimes of four sources have to be measured and compared with each other with an accuracy of approximately $10^{-5}$. An absolute time measurement of decay times in the order of 100 ns would be extremely difficult and unfeasible. By alternate measurements of the decay curve of two chemically different samples it is possible to evaluate the difference of the decay times. Most systematic errors due to non-linearities, drifts etc., which would influence an absolute measurement, will cancel.

The lifetime of the 14.4 keV level ($\tau = 142$ ns) was measured with the coincidence arrangement shown in Figure 3. The principle of the measurement is as follows: A pulse from the 122 keV $\gamma$-quant, which populates the 14.4 keV level, starts a clock. The following 14.4 keV $\gamma$-quant gives the stop signal. As a clock, a time to amplitude converter, T.A.C., was used. A subsequent multichannel pulse height analyser produces a time analysis in the form of a histogram showing the distribution of the analyzed time intervals.

In many respects the decay time of 100 ns is well suited for such measurements. Due to finite rise times, measurements of times shorter than 10 ns require an accurate knowledge of the resolution. Decay time measurements by the coincidence method of $\tau > 1$ $\mu$s are difficult, since chance coincidences, which are proportional to the decay time, limit the source strength and by this the possible statistical accuracy.

The four sources were mounted on the wheel of a sample changer. The reproducibility of the sample positions was within 0.05 mm. As detectors, $1\frac{1}{2}$ in diameter NaI (Tl) crystals mounted on RCA 8575 multipliers were used. The scintillators for the 14.4 keV and 122 keV $\gamma$-rays were 0.2 mm and 25 mm thick. Appropriate absorbers before the 122 keV detector helped to reduce the number of false coincidences due to the escape

of iodine X-rays from the scintillator. The distance between source and detector was approximately 7 mm. Although the decay time constant of NaI(Tl) (250 ns) is very long compared to other scintillators – e.g. naton has a time constant of 2 ns – its much higher light output compensates for this disadvantage. Due to the high counting rates, resulting in large anode currents, the multipliers had to be operated at only 2400 V. Specially designed fast amplifiers (Fig. 4) produced the required additional gain for the anode pulses. The individual photoelectrons cause fluctuations of the anode signal

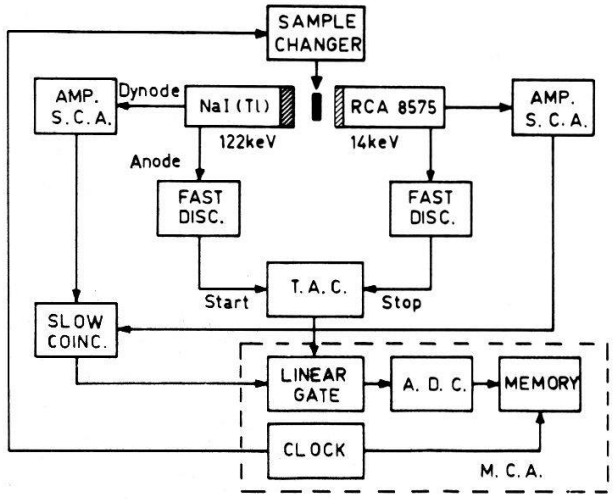


Figure 3
Setup for measuring the influence of the chemical environment on the decay constant of the 14.4 keV $\gamma$-transition in $^{57}Fe$.

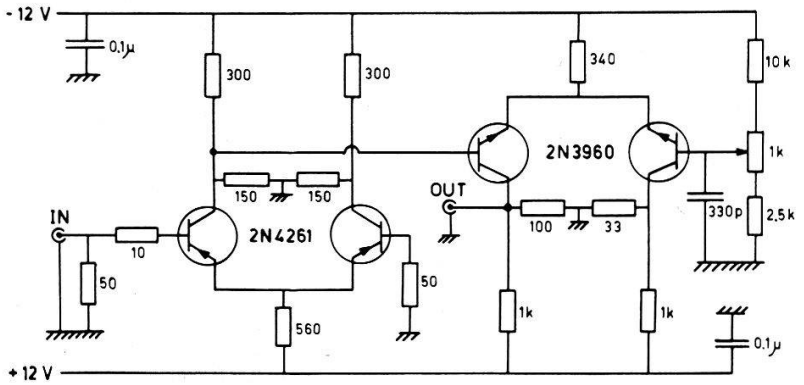


Figure 4
Schematic of the fast amplifiers.

which may result in multiple triggering of the discriminators. This problem, which is typical for the slow NaI(Tl) scintillators, was solved by the use of a stretcher, built into the discriminators. The output signals of the discriminators served as start and stop signal of the T.A.C. (ORTEC 437 A). If within 800 ns after the start pulse a stop pulse arrives the T.A.C. produces an output signal proportional to the time interval to be measured. The energy discrimination done by the single channel analyzers (S.C.A.) and the slow coincidence circuit helped to decrease the number of chance coincidences. The pulses from the T.A.C. were fed via a linear gate to the analog to digital converter (A.D.C.) of a multichannel analyzer (M.C.A.). The time spectra of the four sources were stored in the four quadrants of the memory of the M.C.A. A quartz clock initiated every

5 (10) minutes the advance of the sample changer and memory. During the changes the counting was inhibited. The electronics were temperature stabilized to ±0.3 C. A typical time spectrum accumulated for one of the sources in one day is shown in Figure 5.

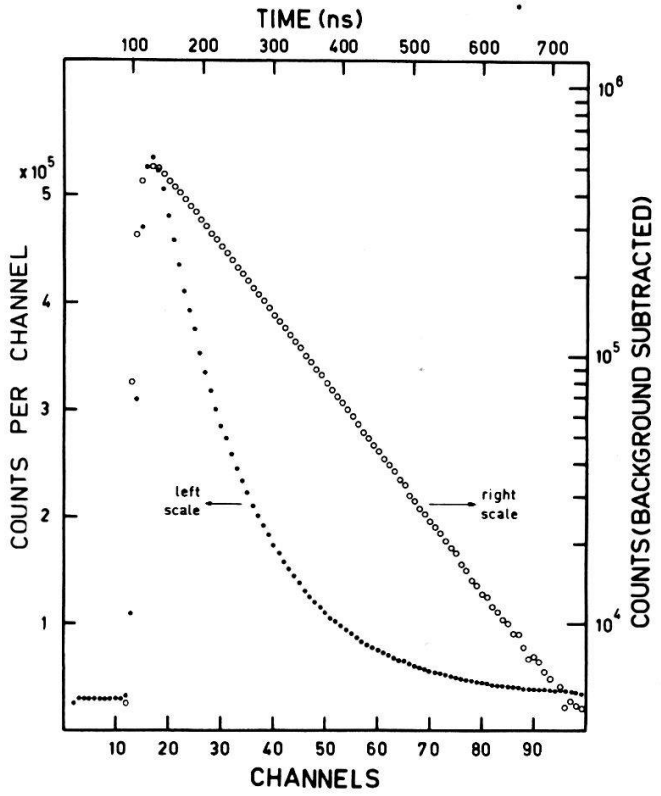


Figure 5
A typical decay curve of the 14.4 keV level of $^{57}$Fe.

The decay curve is due to true ($t$) and random ($r$) coincidences. A random start pulse causes a coincidence in channel $L$ with the probability

$$P_r(L) = n_2 \Delta L \exp(-n_2 L),$$

where $\Delta L$ is the channel width and $n_2 = n_{2r} + n_{2t}$ the stop pulse rate. The factor $e^{-n_2 L}$ takes into account that small time intervals have a higher probability to be recorded than large ones. The probability that a true start leads to a coincidence is

$$P_t(L) = \lambda \exp(-\lambda L) \exp(-n_{2_r} L)\, \Delta L.$$

Since in the experiment $n_{2t}/n_{2r} \approx 10^{-2}$ and $\lambda \gg n_{2r}$ one may write $n_{2r} \cong n_2$. The total number of coincidences are then

$$\begin{aligned} n(L) &= n_{1_r} P_r(L) + n_{1_t} P_t(L) \\ &= (n_{1_r} \cdot n_2 + n_{1_t} \lambda \exp(-\lambda L)) \cdot \exp(-n_2 L)\, \Delta L, \end{aligned}$$

where $n_1$ are the start pulses.

The decay curve was therefore fitted to the function

$$y(L) = (a + b \exp(-\lambda L)) \cdot \exp(-n_2 L). \tag{20}$$

At the beginning the rate of stop pulses was for the Au, Co, Cu and CoO source 27,570, 26,550, 25,540 and 27,680 $s^{-1}$ respectively. The stop rate correction which could be made with an accuracy of $\approx 1\%$ has an influence on the final result ($\Delta\lambda/\lambda$) of approximately 10%.

By starting the evaluation of the spectra approximately 50 ns after the prompt coincidences (channel 23) effects due to the finite resolution of the coincidence circuit and false coincidences from the 8.8 ns level of $^{57}Fe$ (see Fig. 1) could be neglected.

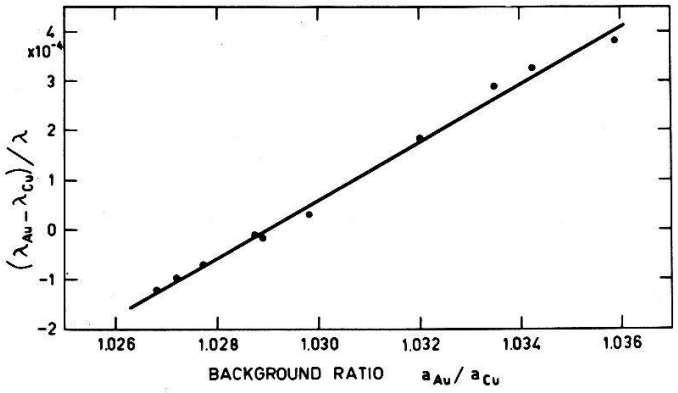


Figure 6
Dependence of $\Delta\lambda/\lambda$ from the background ratio.

The least square fits of the four spectra to equation (20) resulted in fitted values for $a_{Au}$, $a_{Co}$, $a_{Cu}$, and $a_{CoO}$ and $\lambda_{Au}$, $\lambda_{Co}$, $\lambda_{Cu}$, and $\lambda_{CoO}$ respectively. The backgrounds were, in addition, evaluated by averaging the first ten channels of each spectrum ($= a_i'$). One expects that the ratio of the fitted backgrounds $a_i/a_j$ and the ratio of the measured backgrounds $a_i'/a_j'$ agree. By varying the start and stop channel of the fits, it is possible to find a relation between $\Delta\lambda_{ij}/\lambda$ and $a_i/a_j$ for each pair (see Fig. 6). With this relation the fitted values $(\lambda_i - \lambda_j)/\lambda$ were corrected. Differences between the ratios $a_i/a_j$ and $a_i'/a_j'$ were used, as well as the least square fit errors, as indication for the goodness of the individual measurements.

Altogether over one hundred values for each of the six results were averaged with the appropriate weight factor. The six results with the standard deviations are given in Table II.

Table II

Influence of the chemical environment on the decay constant: The measured relative differences of the decay constant $\Delta\lambda/\lambda$ are given for the various source combinations. The negative sign of $\Delta\lambda/\lambda$ indicates a longer lifetime (or smaller electron density at the nucleus) of the 14.4 keV level of $^{57}Fe$ for the first matrix material given in column 1.

| Source combination | $\frac{\Delta\lambda}{\lambda} \times 10^4$ |
|---|---|
| CoO–Co | $-6.3 \pm 1.3$ |
| CoO–Cu | $-4.8 \pm 1.4$ |
| Au–Co | $-4.4 \pm 1.4$ |
| CoO–Au | $-2.2 \pm 1.5$ |
| Au–Cu | $-3.4 \pm 1.5$ |
| Cu–Co | $-1.7 \pm 1.4$ |

*C. Measurement of the isomer shift*

The Mössbauer spectra of the four sources were measured before and after the lifetime measurements. As absorber sodium-ferrocyanide ($Na_4Fe(CN)_6 \cdot 10H_2O$) enriched in $^{57}Fe$ was used (see Figs. 7 and 8). The center shift of the Mössbauer spectra is due to three effects, the IS, the difference of the second-order Doppler effect, and the

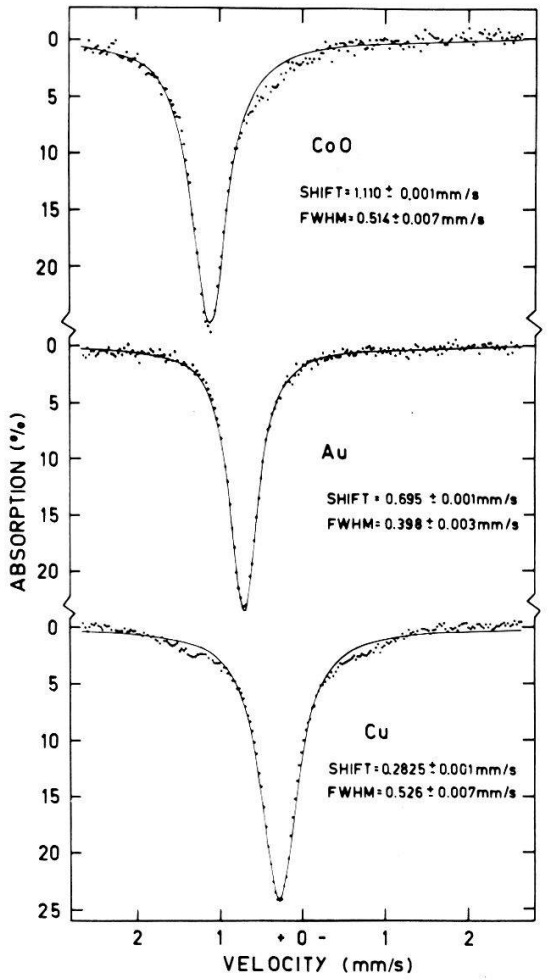


Figure 7
Mössbauer spectra of the three single line sources CoO, Au, and Cu. As absorber 0.5 mg/cm² $^{57}Fe$ in sodium ferrocyanide was used.

negligible small gravitational red shift. For proper IS one has to correct the measured center shifts for the second-order Doppler effect. The second-order Doppler shift is

$$v_{SOD} = -\frac{\langle v^2 \rangle}{2c}, \tag{21}$$

where $\langle v^2 \rangle$ is the mean square velocity of the atom in the solid. In the Debye model $\langle v^2 \rangle$ is expressed by

$$\langle v^2 \rangle = \frac{9k\theta}{8m} + \frac{9kT}{m}\left(\frac{T}{\theta}\right)^3 \int_0^{\theta/T} \frac{x^3\,dx}{e^x - 1}. \tag{22}$$

$\theta$ is the Debye temperature, $kT$ the thermal energy and $m$ the mass of one atom. The corrections for the second-order Doppler shift were determined by measuring the temperature dependence of the center shift. From this dependence the Debye tempera-

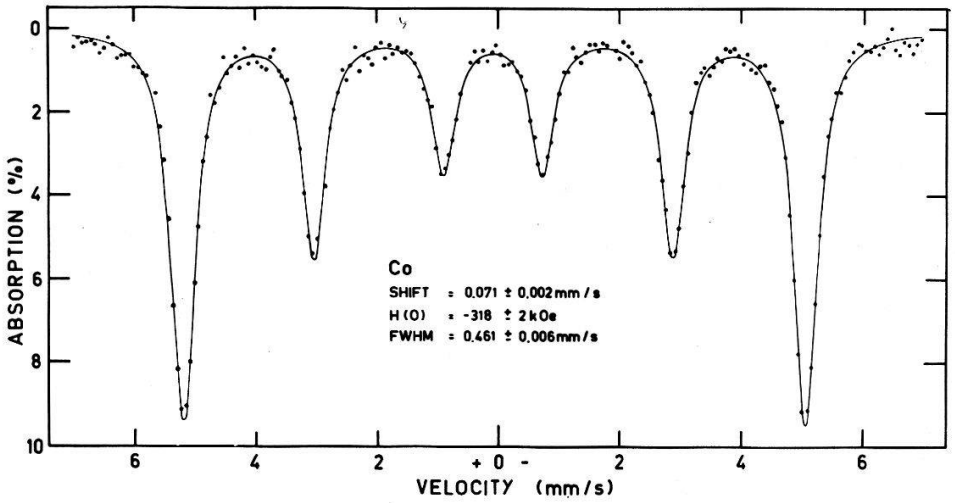


Figure 8
Mössbuaer spectrum of $^{57}$Co diffused into Co.

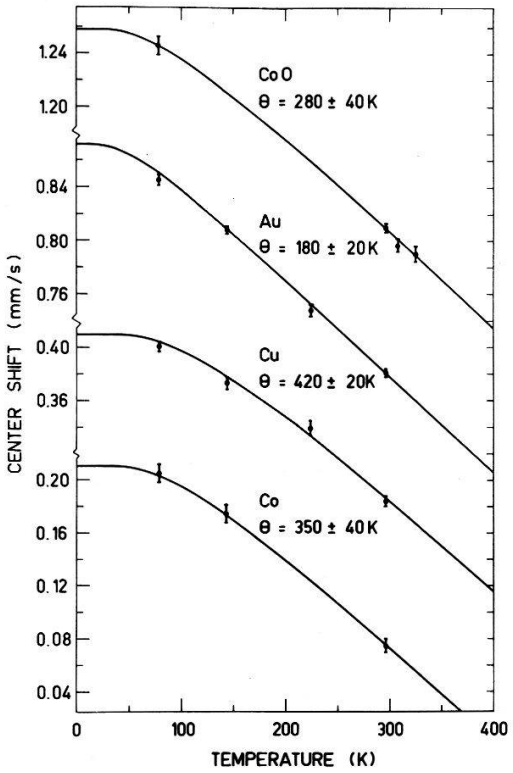


Figure 9
Temperature dependence of the center shift in CoO, Au, Cu, and Co. The curves correspond to the Debye model.

ture for the Fe atom in the various host lattices could be calculated by the use of equations (21) and (22). The result of these measurements with the calculated Debye temperature is shown in Figure 9. The Debye temperatures of Cu and Au are in agreement with values given by Steyert and Taylor [31]. One may attempt to compare the $\theta$ value of CoO I ($\theta = 280$ K) with the value given by Ok and Mullen ($\theta = 510$ K) [28],

a value determined from $f$ measurements. It should be remarked that the Debye temperature determined from shift measurements may be different from $\theta$-values determined from the recoil-free fraction $f$. This is due to the fact that $f$ values are related to the mean square displacement $\langle x^2 \rangle$, which is weighted toward lower frequency phonons than is $\langle v^2 \rangle$. Probably due to the high frequency optical modes of vibration in salts, one finds that Debye temperatures are usually higher for $\langle v^2 \rangle$ data than for

Table III

Determination of the isomer shift from the center shift: The measured center shifts of the Mössbauer spectra had to be corrected for the second-order Doppler shift. The corrections are due to the different Debye temperatures of the sources to be compared. The positive sign of the isomer shift indicates that the first source in the combination (column 1) has the higher $\gamma$-transition energy.

| Source combination | Center shift (mm/s) | Second-order Doppler shift (mm/s) | Isomer shift (mm/s) |
|---|---|---|---|
| CoO–Co | $+1.040 \pm 0.005$ | $-0.006 \pm 0.004$ | $+1.034 \pm 0.007$ |
| CoO–Cu | $+0.827 \pm 0.004$ | $-0.012 \pm 0.003$ | $+0.815 \pm 0.005$ |
| Au–Co | $+0.625 \pm 0.004$ | $-0.011 \pm 0.003$ | $+0.614 \pm 0.005$ |
| CoO–Au | $+0.415 \pm 0.004$ | $+0.006 \pm 0.003$ | $+0.421 \pm 0.005$ |
| Au–Cu | $+0.413 \pm 0.003$ | $-0.013 \pm 0.002$ | $+0.400 \pm 0.004$ |
| Cu–Co | $+0.213 \pm 0.004$ | $+0.007 \pm 0.003$ | $+0.220 \pm 0.005$ |

$\langle x^2 \rangle$ data. Extreme examples of these differences were shown by Lafleur and Goodman [32]. They found, e.g., for potassium ferrocyanide $\theta_{\langle v^2 \rangle} = 716 \pm 40$ K and $\theta_{\langle x^2 \rangle} = 184 \pm 3$ K.

The measured center shifts, the second-order Doppler shift corrections and the IS of the four sources are summarized in Table III.

### *D. The calibration constant*

The proportionality of $\Delta\lambda/\lambda$ and the IS is shown in Figure 10.

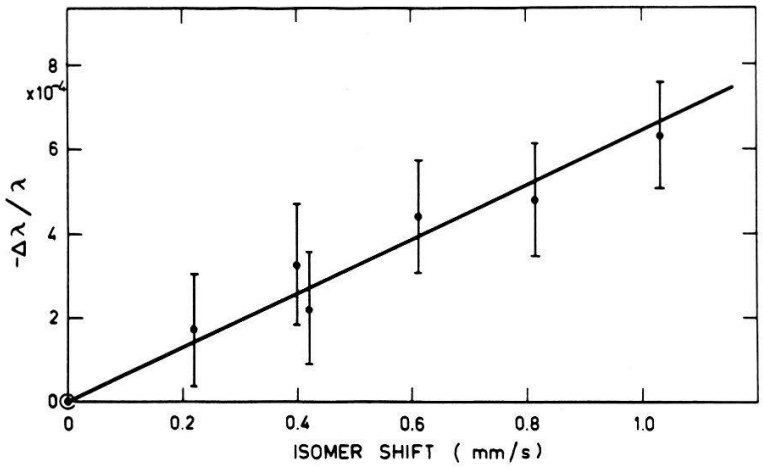


Figure 10
Proportionality of the difference in the decay constant and the isomer shift.

The results of the IS measurements (Table III) and the lifetime measurements (Table III) give, according to equation (10), for the calibration constant,

$$\frac{\Delta R}{R} = -(3.1 \pm 0.5) \cdot 10^{-4}.$$

The error quoted includes the experimental errors (0.32) due to all experimental uncertainties and an estimated systematic error of (0.2) which is mostly due to the uncertainty in $|\psi(0)|^2$.

## Acknowledgments

We wish to express our appreciation for the very helpful discussions with Professor K. Alder and Dr. R. U. Raff. For valuable help in electronics we thank Dr. H. Jung.

REFERENCES

[1] O. C. KISTNER and A. W. SUNYAR, Phys. Rev. Letters *4*, 412 (1960).
[2] R. E. WATSON, *Solid State and Molecular Theory Group*, Techn. Rep. No. 12, Massachusetts Institute of Technology, June 15, 1959.
[3] L. R. WALKER, G. K. WERTHEIM and V. JACCARINO, Phys. Rev. Letters *6*, 98 (1961).
[4] H. WEGENER, *Der Mössbauereffekt und seine Anwendungen in Physik und Chemie* (Hochschultaschenbücher-Verlag Mannheim 1965).
[5] D. A. SHIRLEY, Rev. Mod. Phys. *36*, 339 (1964).
[6] V. I. GOL'DANSKII, *The Mössbauer effect and its applications to chemistry*, At. Energy Rev. *1*, 3 (1963).
[7] J. DANON, *Application of the Mössbauer effect in chemistry and solid state physics*, Techn. Rep. Ser. Intern. At. Energy Agency *50*, 89 (1966).
[8] E. ŠIMÁNEK and Z. ŠROUBEK, Phys. Rev. *163*, 275 (1967).
[9] E. ŠIMÁNEK and A. Y. C. WONG, Phys. Rev. *166*, 348 (1968).
[10] C. J. COSTON, R. INGALLS and H. G. DRICKAMER, J. Appl. Phys. *37*, 1400 (1966).
[11] R. INGALLS, C. J. COSTON, G. DE PASQUALI, H. G. DRICKAMER and J. J. PINAJIAN, J. Chem. Phys. *45*, 1057 (1966).
[12] P. R. CHAMPION, R. W. VAUGHAM and H. R. DRICKAMER, J. Chem. Phys. *47*, 2583 (1967).
[13] T. K. MCNAB, H. MICKLITZ and P. H. BARRETT, Phys. Rev. B *4*, 3787 (1971).
[14] H. MICKLITZ and P. H. BARRETT, Phys. Rev. Letters *28*, 1547 (1972).
[15] F. PLEITER and B. KOLK, Phys. Letters *34B*, 296 (1971).
[16] M. FUJIOKA and K. HISATAKE, Phys. Letters *40B*, 99 (1972).
[17] B. FRICKE and J. T. WABER, Phys. Rev. B *5*, 3445 (1972).
[18] H. J. MANG, J. MEYER, J. SPETH and W. WILD, Phys. Letters *32B*, 321 (1970).
[19] G. M. KALVIUS, in *Hyperfine Interactions in Excited Nuclei*, edited by G. GOLDRING and R. KALISH (Gordon and Breach Science Publ., New York 1971), p. 523.
[20] H. C. PAULI, Nucl. Phys. *A109*, 94 (1968).
[21] U. RAFF, K. ALDER and G. BAUR, Helv. Phys. Acta *45*, 427 (1972).
[22] H. U. FREUND and J. C. MCGEORGE, Z. Physik *238*, 6 (1970).
[23] D. P. Johnson, Phys. Rev. B *1*, 3551 (1970).
[24] L. R. B. ELTON and A. SWIFT, Proc. Phys. Soc. (London) *84*, 125 (1964).
[25] M. ECKHAUSE, R. J. HARRIS, JR., W. B. SHULER and R. E. WELSH, Proc. Phys. Soc. (London) *89*, 187 (1966).
[26] C. HOHENEMSER, R. RENO, H. C. BENSKI and J. LEHR, Phys. Rev. *184*, 298 (1969).
[27] F. J. LYNCH, R. E. HOLLAND and M. HAMERMESH, Phys. Rev. *120*, 513 (1960).
[28] D. P. JOHNSON, Phys. Rev. B *1*, 3551 (1970).
[29] L. YAFFE, Ann. Rev. Nucl. Sci. *12*, 177 (1962).
[30] H. N. OK and J. G. MULLEN, Phys. Rev. *168*, 550 (1968).
[31] W. A. STEYERT and R. D. TAYLOR, Phys. Rev. A *134*, 716 (1964).
[32] L. D. LAFLEUR and C. GOODMAN, Phys. Rev. B *4*, 2915 (1971).